Forbidden Electronic Transitions between the Singlet Ground State and the Triplet Excited State of Pt(II) Complexes

Greg Y. Zheng,[†] D. Paul Rillema,*[,†] Jeff DePriest,[‡] and Clifton Woods[‡]

Departments of Chemistry, University of Tennessee, Knoxville, Tennessee 37996, and Wichita State University, Wichita, Kansas 67260

Received March 24, 1998

Direct access to the triplet emitting state from the ground state is observed for Pt(II) complexes containing heterocyclic (C∧C′, C∧N, N∧N′) and bis(diphenylphosphino)alkane (P∧P′) ligands. Extinction coefficients for such transitions are in the range 4−25 M^{-1} cm^{-1}. Emission quantum yields resulting from singlet-to-triplet excitation are as high as 61−77 times the emission quantum yields resulting from singlet-to-singlet excitation at 296 K. The intersystem crossing quantum yield from the singlet excited state to triplet emitting state is lower than 2% at 296 K but is greatly enhanced at 77 K. The forbidden electronic transition observed for Pt(II) complexes is attributed to result from spin−orbit coupling due to the presence of Pt(II) in the skeleton structure. The importance of excitation spectra on the computation of emission quantum yields is discussed.

Introduction

We are currently studying the photophysical properties of a series of square planar Pt(II) complexes[1−6] containing heterocyclic and bis(diphenylphosphino)alkane ligands (Figure 1). On the basis of emission spectra and emission lifetimes, the emitting state in dilute solution has been assigned as a metal perturbed ^{3}LC state. Since luminescence occurs from the triplet excited state to the singlet ground state, the corresponding transition from the singlet ground state to the triplet excited state should, at least in principle, be observed. Transitions with low absorption coefficients in the visible spectrum were observed for 2-phenylpyridine (2-phpy) platinum(II) complexes,[7−9] and a transition for $[Pt(2\text{-phpy})Cl_2]^-$ located at 488 nm was assigned to direct population of the triplet excited state from the singlet ground state.[9] Details regarding the transition were not explored.

Several features relate to singlet-to-triplet ($S_0 \rightarrow T_1$) transitions. First, the position of the 0−0 band for $S_0 \rightarrow T_1$ absorption should be nearly identical to that of the 0−0 band for triplet-to-singlet ($T_1 \rightarrow S_0$) emission, or a very small Stokes shift should exist. Second, an approximately mirror image relationship between the $S_0 \rightarrow T_1$ absorption profile and $T_1 \rightarrow S_0$ emission profile is expected. Third, the intensity of the $S_0 \rightarrow T_1$ absorption, a spin-forbidden transition, is expected to be weak with a small extinction coefficient compared to spin-allowed absorptions. Fourth, identical emission profiles are expected from both spin-forbidden and spin-allowed excitations when the origin of emission is from the same state.

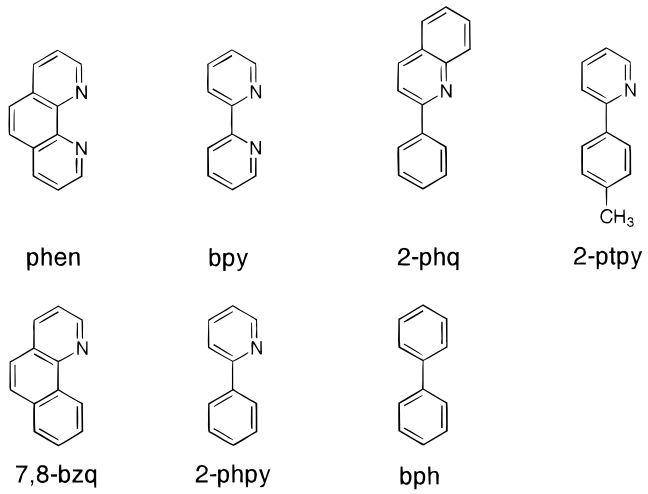

Figure 1. The C∧C′, C∧N, and N∧N′ ligands.

The $S_0 \rightarrow T_1$ absorption spectra were studied by regular absorption and excitation spectra methods. Due to small extinction coefficients, $S_0 \rightarrow T_1$ absorptions are normally masked by other more intense transitions or are simply too weak to be observed. But for our Pt(II) complexes, the $S_0 \rightarrow T_1$ absorptions were observed by both absorption and excitation methods. This paper focuses on the benefits of direct excitation to the triplet state from the ground state.

Experimental Section

Materials. The preparation, purification, and characterization for most of the platinum(II) compounds and their precursors were described previously.[4,6,10] Methylene chloride and methanol were optima grade

* To whom correspondence should be addressed.
† Wichita State University.
‡ University of Tennessee.

(1) Blanton, C. B.; Murtaza, Z.; Shaver, R. J.; Rillema, D. P. *Inorg. Chem.* **1992**, *31*, 3230.
(2) Blanton, C. B.; Rillema, D. P. *Inorg. Chim. Acta* **1990**, *168*, 145.
(3) Chen, Y. H.; Merkert, J. W.; Murtaza, Z.; Woods, C.; Rillema, D. P. *Inorg. Chim. Acta* **1995**, *240*, 41.
(4) DePriest, J.; Zheng, G. Y.; Woods, C.; Rillema, D. P.; Mikirova, N. A.; Zandler, M. E. *Inorg. Chim. Acta* **1997**, *264*, 287.
(5) Zheng, G. Y.; Rillema, D. P. *Inorg. Chem.* **1998**, *37*, 1392.
(6) DePriest, J.; Zheng, G. Y.; Woods, C.; Rillema, D. P. Inorg. Chem., submitted for publication.
(7) Chassot, L.; Muller, E.; von Zelewsky, A. *Inorg. Chem.* **1984**, *23*, 4249.
(8) Chassot, L.; von Zelewsky, A. *Inorg. Chem.* **1987**, *26*, 2814.
(9) Craig, C. A.; Garces, F. O.; Watts, R. J.; Palmans, R.; Frank, A. J. *Coord. Chem. Rev.* **1990**, *97*, 193.
(10) Wan, K.-T.; Che, C.-M. *J. Chem. Soc., Chem. Commun.* **1990**, 140.

S0020-1669(98)00324-3 CCC: $15.00
Published on Web 06/19/1998

and purchased from Fisher Scientific. The ligands 2,2′-bipyridine and 1,10-phenanthroline and NH_4PF_6 were purchased from Aldrich Chemical Co. Absolute ethanol was purchased from McCormick Distilling Co. Ethanol and methanol were used in a 4:1 (v/v) mixture to prepare the solutions for emission studies.

Preparation of Compounds. (a) Pt(dppe)$(NO_3)_2$. Pt(dppe)$(NO_3)_2$ was prepared by the addition of $AgNO_3$ (0.171 g, 1.01 mmol) in 5 mL of water to a rapidly stirred solution of Pt(dppe)Cl_2 (0.290 g, 0.436 mmol) in 200 mL of CH_2Cl_2 contained in a flask wrapped with aluminum foil. After 5 min, the water layer became opaque. Sufficient acetone was added (200 mL) until the liquids emulsified. After the resulting AgCl suspension stirred for 30 min, the AgCl was removed by filtration. Isolation of the product was not attempted. The completeness of conversion of the dichloride to the dinitrato species was verified in each synthesis by using $^{31}P\{^1H\}$ NMR. The chemical shift and coupling constant were not altered by the presence of water in the CH_2Cl_2.

(b) Pt(dppp)$(NO_3)_2$. Pt(dppp)$(NO_3)_2$ was prepared from Pt(dppp)-Cl_2 (0.497 g, 0.733 mmol) and $AgNO_3$ (0.337 g, 1.99 mmol) by the same procedure used to prepare Pt(dppe)$(NO_3)_2$. Isolation of the product was not attempted. The completeness of conversion of the dichloride to the dinitrato species was verified in each synthesis by using $^{31}P\{^1H\}$ NMR. The chemical shift and coupling constant were not altered by the presence of water in the CH_2Cl_2.

(c) [Pt(bpy)(dppe)]$(PF_6)_2$. The ligand 2,2′-bipyridine (0.0972 g, 0.622 mmol) was introduced into the light yellow acetone/CH_2Cl_2 solution of Pt(dppe)$(NO_3)_2$ prepared as outlined above. Addition of NH_4PF_6 (1.00 g, 6.15 mmol) followed by rotary evaporation to reduce the volume of the solvent resulted in the isolation of a white solid. [Pt(bpy)(dppe)]$(PF_6)_2$ decomposed upon exposure to silica gel in both CH_2Cl_2 and acetone solutions. Hence, purification was achieved by stripping the crude reaction mixture containing excess NH_4PF_6 to dryness and extracting the product with 3 × 30 mL portions of CH_2Cl_2. (NH_4PF_6 is insoluble in CH_2Cl_2.) The CH_2Cl_2 extracts were combined and reduced to 30 mL. Then 100 mL of ethanol and 30 mL of hexanes were added, and the resulting solution was allowed to stand undisturbed (several hours) until small colorless crystals emerged. Several successive crops of crystals were obtained, and each crop was evaluated for purity by $^{31}P\{^1H\}$ NMR. (The area of the peaks for [Pt(bpy)-(dppe)]$^{2+}$ to PF_6^- must equal 1:1.) Finally, the product was recrystallized from acetone by adding anhydrous diethyl ether until precipitation was complete. The product, a white solid, was dried in vacuo. The yield was 24% (0.2548 g). Elemental Anal. Calcd for [Pt(bpy)(dppe)]$(PF_6)_2$: C, 41.59; H, 3.10. Found: C, 41.41; H, 2.91. Vis/UV spectra, λ_{max} (nm) [$\epsilon \times 10^{-3}$ (cm^{-1}, M^{-1})]: 336 (8.77 ± 0.21), 320 (12.7 ± 0.3), 275 (33.9 ± 1.2).

(d) [Pt(phen)(dppe)]$(PF_6)_2$. [Pt(phen)(dppe)]$(PF_6)_2$ was prepared by the same procedures used to synthesize [Pt(bpy)(dppe)]$(PF_6)_2$. The Pt(dppe)$(NO_3)_2$ solution was prepared using Pt(dppe)Cl_2 (0.843 g, 1.27 mmol) and $AgNO_3$ (0.508 g, 2.96 mmol). The ligand 1,10-phenanthroline (0.416 g, 2.31 mmol) was added to the solution followed by NH_4PF_6 (2.213 g, 13.6 mmol), and reduction in volume of the solvent by rotary evaporation yielded a white precipitate. The solid was recrystallized twice from acetone/diethyl ether and dried in vacuo. The yield was 89% (0.401 g). Elemental Anal. Calcd for [Pt(phen)(dppe)]-$(PF_6)_2$: C, 42.91; H, 3.03. Found: C, 42.96; H, 3.15. Vis/UV spectra, λ_{max} (nm) [$\epsilon \times 10^{-3}$ (cm^{-1}, M^{-1})]: 360 (1.79 ± 0.04), 341 (2.46 ± 0.04), 331 (4.18 ± 0.06), 286 (32.4 ± 0.8), 277 (33.2 ± 0.9).

(e) [Pt(bpy)(dppp)]$(PF_6)_2$. The preparative procedure followed the one for the preparation of [Pt(bpy)(dppe)]$(PF_6)_2$. The ligand 2,2′-bipyridine (0.341, 2.18 mmol) was added to the solution of Pt(dppp)-$(NO_3)_2$ prepared as outlined above. Introduction of NH_4PF_6 (1.26 g, 7.76 mmol) and reduction in volume of the solvent by rotary evaporation yielded a light yellow solid which was recrystallized twice from acetone/diethyl ether and dried under vacuum. The yield was 99% (0.76 g). Elemental Anal. Calcd for [Pt(bpy)(dppp)]$(PF_6)_2$: C, 42.18; H, 3.25. Found: C, 42.22; H, 2.99. Vis/UV spectra, λ_{max} (nm) [$\epsilon \times 10^{-3}$ (cm^{-1}, M^{-1})]: 335 (7.26 ± 0.13), 322 (10.2 ± 0.3), 302 (15.6 ± 0.6), 291 (19.1 ± 0.2), 277 (21.5 ± 0.3).

(f) [Pt(phen)(dppp)]$(PF_6)_2$. [Pt(phen)(dppp)]$(PF_6)_2$ was prepared by the same procedures used to synthesize [Pt(bpy)(dppe)]$(PF_6)_2$. The Pt(dppp)$(NO_3)_2$ solution was prepared using Pt(dppp)Cl_2 (0.441 g, 0.694 mmol) and $AgNO_3$ (0.367 g, 2.16 mmol). The ligand 1,10-phenanthroline (0.452 g, 2.51 mmol) was added to the solution followed by NH_4PF_6 (1.16 g, 7.12 mmol), and reduction in volume of the solvent by rotary evaporation yielded a white precipitate. The solid was recrystallized twice from acetone/ether and dried in vacuo. The yield was 36% (0.250 g). Elemental Anal. Calcd for [Pt(phen)(dppp)]$(PF_6)_2$: C, 43.47; H, 3.18. Found: C, 43.19; H, 2.95. Vis/UV spectra, λ_{max} (nm) [$\epsilon \times 10^{-3}$ (cm^{-1}, M^{-1})]: 361 (1.63 ± 0.04), 343 (2.31 ± 0.06), 330 (4.34 ± 0.06), 286 (36.5 ± 3.6), 277 (35.9 ± 6.5).

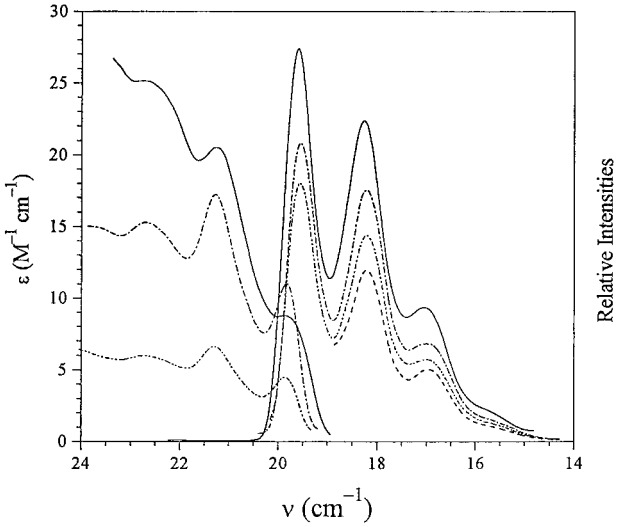

Figure 2. Absorption spectra: (—) absorption spectrum in CH_2Cl_2 at 296 K, left *y* axis is used; (— · —) excitation spectrum (detected at 548 nm) in 4:1 (v/v) EtOH/MeOH at 77 K, right *y* axis is used; (— ·· —) excitation spectrum (detected at 587 nm) in 4:1 (v/v) EtOH/MeOH at 77 K, right y axis is used. Emission spectra measured in 4:1 (v/v) EtOH/MeOH at 77 K, right *y* axis is used: (—) excited at 353 nm; (— · —) excited at 440 nm; (— ·· —) excited at 470 nm; (---) excited at 504 nm.

Physical Measurements. UV/visible spectra were recorded with a double-beam Cary 14 spectrophotometer modified with an Olis automation package, and corrected emission spectra were obtained with a Spex 212 Fluorolog spectrofluorometer. The visible absorption spectra were measured in CH_2Cl_2 at 296 K. Samples for emission studies were prepared in a mixed solvent of 4:1 (v/v) C_2H_5OH/CH_3OH and were degassed by at least three freeze−pump−thaw cycles prior to the measurements. Low- and room-temperature emission spectra were obtained by excitation at the singlet-to-singlet and singlet-to-triplet transitions.

Emission quantum yields were measured at 296 K. The standard used was Rhodamine B ($\phi_r = 0.71$), and eq 1 was used to calculate the

$$\phi_s = \phi_r \left(\int I_s(\nu)\, d\nu / \int I_r(\nu)\, d\nu\right)(I_r^0/I_s^0)\{(1 - e^{-2.3A_r})/(1 - e^{-2.3A_s})\} \quad (1)$$

emission quantum yields.[11] In eq 1, ϕ_s is the emission quantum yield of the sample, ϕ_r is the emission quantum yield of the reference, A_s and A_r are the absorbance of the sample and reference, respectively, $\int I_s(\nu)\, d\nu$ and $\int I_r(\nu)\, d\nu$ are integrals under the emission spectra of sample and reference, respectively, and I_s^0 and I_r^0 are incident light intensities at the excitation wavelength. Samples and standard were prepared with absorbances at the excitation wavelength of less than 0.1 to minimize self-absorption.

Results

Absorption, Excitation, and Emission Spectra. Figure 2 shows an absorption spectrum in CH_2Cl_2 at 296 K for Pt(bph)-

(11) Demas, J. N.; Crosby, G. A. *J. Phys. Chem.* **1971**, *75*, 991.

Table 1. Absorption and Emission Properties between Ground Singlet and Excited Triplet States at 77 and 296 K[a,c]

	296 K	77 K				
	$E(^1S_0 \rightarrow {}^3T_1)$ (10^3 cm^{-1})	$E(^1S_0 \rightarrow {}^3T_1)$ (10^3 cm^{-1})	$E(^3T_1 \rightarrow {}^1S_0)$ (10^3 cm^{-1})	$\phi_{P,T}/\phi_{P,S}$[d]	τ (μs)	Stokes shift[b]
Pt(bph)(dppm)	19.72(9.3), +1.47(21.9), +2.80(25.5)	19.84, +1.44, +2.89	19.61, −1.36, −2.57	14, 6, 5	16.7	0.23
[Pt(phpy)(dppm)]$^+$	21.05(6.7), +1.52(14.4)	21.19, +1.56, +2.62	20.98, −1.45, −2.56	4, 3	47.6	0.21
[Pt(ptpy)(dppm)]$^+$	20.75(5.7), +1.47(11.6)	20.90, +1.52, +2.77	20.62, −1.46, −2.50	8, 5	60.6	0.28
[Pt(phq)(dppm)]$^+$	19.38(6.9), +1.37(12.3)	19.34, +1.38, +2.64	19.01, −1.40, −2.70	13, 6	54.9	0.33
[Pt(bzq)(dppm)]$^+$	21.41(17.2)	21.63, +1.63	21.28, −1.40, −2.80	2	204	0.35
[Pt(bzq)(dppe)]$^+$	21.60(9.1)	21.74	21.19, −1.43, −2.81	12		0.55
[Pt(bzq)(dppp)]$^+$	21.65(8.8)	21.83, +1.64	21.19, −1.43, −2.81	7		0.64
[Pt(bpy)(dppm)]$^{2+}$	na[e]	22.52	21.99, −1.46, −2.57	na	27	0.53
[Pt(bpy)(dppe)]$^{2+}$	22.52(2.4), +1.46(4.9)	22.52, +1.54, +3.12	22.12, −1.54, −2.49	5, 5		0.40
[Pt(bpy)(dppp)]$^{2+}$	21.65(8.8)	22.62, +1.65	22.17, −1.51, −2.60	2		0.45
[Pt(phen)(dppm)]$^{2+}$	23.53(4.8)	23.75	22.17, −1.42, −2.79	5	1170	1.58
[Pt(phen)(dppe)]$^{2+}$	23.75(4.1)	23.70	21.98, −1.40, −2.79	6		1.72
[Pt(phen)(dppp)]$^{2+}$	na	23.81	22.22, −1.43, −2.80	na		1.59

[a] dppm, bis(diphenylphosphino)methane-P,P′; dppe, 1,2-bis(diphenylphosphino)ethane-P,P′; dppp, 1,3-bis(diphenylphosphino)propane-P,P′; bph, biphenyl-C,C′; phpy, 2-phenylpyridine-N,C; ptpy, 2-(*p*-toluene)pyridine-N,C; phq, 2-phenylquinoline-N,C; bzq, 7,8-benzoquinoline-N,C; bpy, 2,2′-bipyridine-N,N′; phen, 1,10-phenanthroline-N,N′. [b] Stokes shift is the difference between the lowest energy absorption band and the highest energy emission band at 77 K. [c] Errors in measured energies are less than 0.05 kK. Values in parentheses are extinction coefficients in M^{-1} cm^{-1}. [d] $\phi_{P,T}/\phi_{P,S} = \phi_{isc}^{-1}$. [e] na, not available.

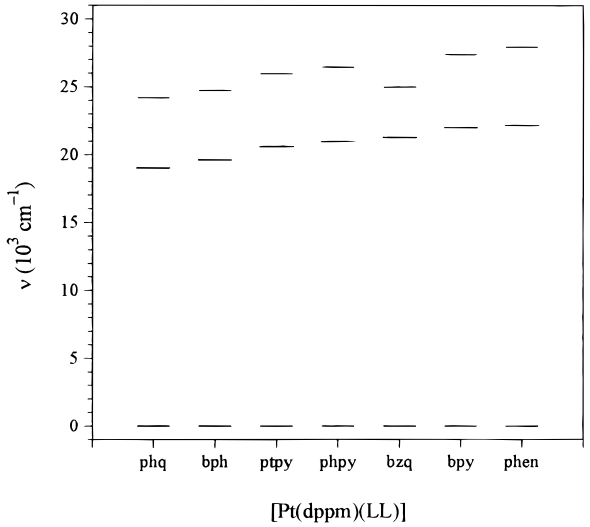

Figure 3. Relative energy map: lower line, ground state; middle line, triplet excited state; upper line, singlet excited state.

(dppm), where bph is the biphenyl dianion and dppm is bis-(diphenylphosphino)methane. Its emission spectra at 77 K in a 4:1 (v/v) C_2H_5OH/CH_3OH glass excited at both the $S_0 \rightarrow S_1$ and the $S_0 \rightarrow T_1$ transitions, and its excitation spectra at different observation wavelengths in the glass at 77 K are also included in Figure 2.

Results for Pt(bph)(dppm) and other Pt(II) complexes studied are given in Table 1. The emission band with the highest energy maximum is given, followed by the relative positions of other band maximums with respect to the highest energy band. The negative sign indicates the band maximums progressed toward the red. The absorption band with the lowest energy maximum is given for both absorption and excitation spectra, followed by the relative positions of other band maximums with respect to the lowest energy band. The positive sign indicates the bands progressed toward the blue. The lowest energy $S_0 \rightarrow S_1$ absorption band is assigned on the basis of its position and separation from the assigned highest energy $S_0 \rightarrow T_1$ absorption band. The relative energies of the singlet and triplet excited states together with their vibrational levels are mapped in Figure 3. Stokes shifts, which represent the displacement of the emitting state potential surface manifold with respect to the ground-state manifold, ranged from 230 to 1720 cm^{-1}.

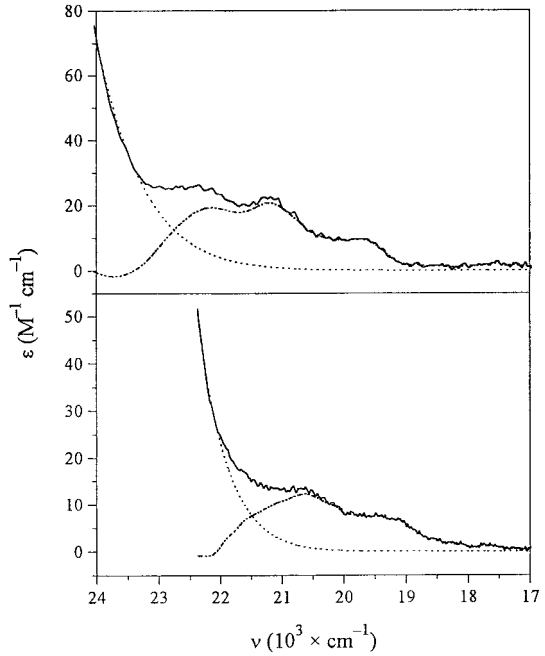

Figure 4. $^1S_0 \rightarrow {}^3T_1$ absorption spectra: top, Pt(bph)(dppm); bottom, Pt(phq)(dppm)(PF_6). (—) spectra from experiment; (---) corrected baselines; (— ·· —) spectra after correction.

Emission Quantum Yields and Their Ratios. Emission quantum yields for Pt(bph)(dppm), excited at 342 nm, and [Pt(2-phq)(dppm)]PF_6, where 2-phq is 2-phenylquinoline, excited at 396 nm, were found to be 1.5×10^{-3} and 1.5×10^{-4} in 4:1 (v/v) C_2H_5OH/CH_3OH at 296 K, respectively. Such emission quantum yields resulting from higher energy photon excitation were assigned as $\phi_{P,S}$, which represents an emission quantum yield resulted from singlet-to-singlet excitation. Emission quantum yields resulting from $S_0 \rightarrow T_1$ excitation were evaluated by eq 2, where $\phi_{P,T}$ and $\phi_{P,S}$ are the emission quantum yields

$$\phi_{P,T}/\phi_{P,S} = (\int I_{P,T}(\nu)\, d\nu / \int I_{P,S}(\nu)\, d\nu)(I_S^0/I_T^0)\{(1 - e^{-2.3A_s})/(1 - e^{-2.3A_T})\} \quad (2)$$

resulting from $S_0 \rightarrow T_1$ excitation and $S_0 \rightarrow S_1$ excitation, respectively, and are defined as $\phi_P = I_P/(2.3I^0\epsilon cl)$. I^0 is the incident light intensity at the excitation wavelength, A is the

absorbance at the excitation wavelength, and $\int I_{P,T}(\nu)\, d\nu$ is the integral under the emission spectrum of interest. Equation 2 was further simplified to eq 3, where ϕ_λ is the emission quantum

$$\phi_{\lambda 1}/\phi_{\lambda 2} = (I_{\lambda 1}/I_{\lambda 2})(I_{\lambda 2}{}^0/I_{\lambda 1}{}^0)(\epsilon_{\lambda 2}/\epsilon_{\lambda 1}) \quad (3)$$

yield resulting from excitation at λ; I_λ is the intensity obtained from the excitation spectrum at λ, $I_\lambda{}^0$ is the incident light intensity at λ, and ϵ_λ is the molar extinction coefficient at λ. From eq 3, the relative emission quantum yields resulting from excitation at λ_1 and λ_2 were computed from a single excitation spectrum. The validation of eq 3 was tested for several compounds and compared with results from eq 2. The difference was less than 1%.

From eq 3 and the measured emission quantum yields resulting from singlet-to-singlet excitation, quantum yields ($\phi_{P,T}$) resulting from $S_0 \rightarrow T_1$ can then be computed. Values of 0.12 for Pt(bph)(dppm) excited at 476 nm and 9.1×10^{-3} for [Pt(phq)(dppm)]PF_6 excited at 488 nm were obtained, an enhancement of 77 and 61, respectively.

Emission quantum yield ratios of $S_0 \rightarrow T_1$ to $S_0 \rightarrow S_1$ excitations can be related to the intersystem crossing quantum yield, ϕ_{isc},

$$\phi_{P,S} = (\phi_{isc})\tau k_r = (\phi_{isc})(\phi_{P,T}) \quad (4)$$

or

$$\phi_{isc}{}^{-1} = \phi_{P,T}/\phi_{P,S} \quad (5)$$

The emission quantum yield ratios ($\phi_{isc}{}^{-1}$), which compare the efficiency of $S_0 \rightarrow T_1$ excitation ($\phi_{P,T}$) to $S_0 \rightarrow S_1$ MLCT excitation ($\phi_{P,S}$) at 77 K, were computed by eq 3 and are given in Table 1. Molar extinction coefficients measured at 296 K were used in these computations.[12]

Discussion

The Transition between S_0 and T_1. As shown in Figure 2, the emission profiles[9] are identical to each other regardless of the excitation energy and lead to several points. First, excitation at the lowest energy transition leads to the same emitting state as excitation at the $S_0 \rightarrow S_1$ transition. Second, the excitation spectra are nearly mirror images of the emission spectra with similar vibronic progressions. Third, the small Stokes shift implies direct excitation to the emitting state. And fourth, the small extinction coefficients, 4−25 M^{-1} cm^{-1} (compared to extinction coefficients of 10^3−10^4 M^{-1} cm^{-1} for the spin-allowed $S_0 \rightarrow S_1$ transitions[1−6]), are consistent with a spin-forbidden transition and in agreement with those obtained for $S_0 \rightarrow T_1$ transitions, 60−100 M^{-1} cm^{-1}, reported for other Pt(II) complexes.[7−9] The possibility of attributing the assigned $S_0 \rightarrow T_1$ transitions to d−d transitions can be excluded due to strong field ligands, bidentate aromatic (C∧C′, C∧N, N∧N′), and bis(diphenylphosphino)alkane ligands, coordinated to Pt(II). Such strong field ligands almost certainly cause large d−d splittings; hence, d−d transitions are not expected to be observed in the spectral region found for the $S_0 \rightarrow T_1$ absorptions. Therefore, the assignment of the low-energy transition as a $S_0 \rightarrow T_1$ transition is quite conclusive.

The positions of the bands listed in Table 1 attributed to $S_0 \rightarrow T_1$ absorption measured for Pt(bph)(dppm) in CH_2Cl_2 at 296 K were similar in energy to those observed from excitation spectra at 77 K. The reason for this may be due to offsetting effects of temperature and the matrix. Lower temperatures tend to shift emission spectra to higher energy, whereas shifts to lower energy occur in solution compared to the glassy matrix.

The observed spin-forbidden transition to the triplet state can be explained by spin−orbit coupling, in which the orbital angular momentums are added to the spin angular momentums. The enhancement of spin−orbit coupling by a heavy atom or ion increases the probability of $S_0 \rightarrow T_1$ transition. Thus, the introduction of Pt(II) into the skeleton of the complexes removes the distinctiveness of the spin momentums, breaks down the spin conservation rule, facilitates a change in multiplicity, and permits weak $S_0 \rightarrow T_1$ absorption. In other words, spin−orbit coupling mixes one electronic state with another resulting in increased transition moments by coupling different electronic states through spin−orbit interaction.[13]

The extent of mixing of two states due to spin−orbit coupling depends inversely on the energy separation of the two states.[14] The smaller the separation, the greater the mixing of the states. By adjusting the chromophoric and/or nonchromophoric ligands, the relative positions of singlet and triplet excited states with respect to the singlet ground state can be tuned and the efficiencies of the intersystem crossing transitions can be varied. The greater mixing of the triplet excited-state with the singlet excited state enhances the efficiency of intersystem crossing making the triplet state readily accessible from the singlet excited state. The result may be a longer lived excited state. The mixing of the triplet excited state with the singlet ground state enhances the $S_0 \rightarrow T_1$ absorption and the $T_1 \rightarrow S_0$ decay to the ground state. A shorter lived excited state is then expected.

As shown in Figure 3, Pt(bph)(dppm) and Pt(7,8-bzq)(dppm)-(PF_6), where bzq is 7,8-benzoquinoline, have similar $S_0 \rightarrow S_1$ transition energies but different emitting state energies. The energy difference between S_1 and T_1 states is smaller for Pt(7,8-bzq)(dppm)(PF_6). Thus, the emitting state for Pt(7,8-bzq)-(dppm)(PF_6) would mix more with its singlet excited state but less with the ground state, whereas the opposite would occur for Pt(bph)(dppm). One would expect a higher intersystem crossing quantum yield and longer lifetime (204 μs) for Pt(7,8-bzq)(dppm)(PF_6) than that (16.7 μs) for Pt(bph)(dppm). The results in Table 1 are in agreement with this. Further comparison between Pt(2-phq)(dppm)(PF6), Pt(bph)(dppm), Pt(2-ptpy)-(dppm)(PF_6), and Pt(2-phpy)(dppm)(PF_6), where 2-ptpy is 2-(*p*-toluene)pyridine, shows that the energy differences between the singlet excited state and the emitting state are about the same, but the energy differences between emitting states and the ground states increase in the order of 2-phq < bph < 2-ptpy < 2-phpy. As shown in Table 1, the intersystem crossing quantum yield increases in this order, but the change in the lifetime does not follow the same trend.

The vibronic progressions for emission spectra correspond to different vibronic levels in the singlet ground state; the vibronic progressions for excitation spectra correspond to different vibronic levels in the triplet excited state. A small Stokes shift implies that the triplet manifold is almost vertically displaced above the ground-state energy manifold. Such an arrangement makes more vibrational levels of the excited states

(12) Ratios can be regarded as estimates. If the ϵ changes are the same, then the ratios are correct. If ϵ for the $S_0 \rightarrow S_1$ absorption increases more than ϵ for the $S_0 \rightarrow T_1$ absorption, then the ratios are lower limits, or vice versa, the ratios will be upper limits if ϵ for the $S_0 \rightarrow T_1$ absorption increases more than ϵ for the $S_0 \rightarrow S_1$ absorption.

(13) Balasubramanian, K. *J. Phys. Chem.* **1989**, *93*, 6585.
(14) Becker, R. S. *Theory and Interpretation of Fluorescence and Phosphorescence;* Wiley: New York, 1969.

Table 2. Calculated Radiative Rate Constants at 296 K from Eq 6

	solvent	n^2	$\int\epsilon\ \mathrm{d}\ln\nu$	$<\nu_e^{-3}>_{A\upsilon}^{-1}$	k_r (s^{-1})	$\phi_{T,P}$	τ (ns) [3]	k_r' (s^{-1})[a]
Pt(bph)(dppm)	CH_2Cl_2	2.03	2.68	6.09×10^{12}	3.2×10^4	0.12	25	4.8×10^6
Pt(phq)(dppm)(PF_6)	CH_2Cl_2	2.03	1.44	5.58×10^{12}	1.6×10^4	9.1×10^{-3}	3.8	2.4×10^6

[a] Calculated from $k_r = \tau^{-1}\phi_{em}$.

accessible by $S_0 \rightarrow T_1$ absorption and a more structured profile. As shown in Table 1, a small Stokes shift of 230 cm^{-1} for Pt(bph)(dppm) gave rise to a highly structured $S_0 \rightarrow T_1$ absorption spectrum. The larger Stokes shift of 1720 cm^{-1} for [Pt(phen)(dppe)]$(PF_6)_2$, where phen is 1,10-phenanthroline and dppe is 1,2-bis(diphenylphosphino)ethane, on the other hand, resulted in the observation of only a single $S_0 \rightarrow T_1$ absorption band. The larger Stokes shift implies that the triplet manifold is displaced from the vertical position above the ground-state energy manifold making fewer lower energy vibrational levels of the excited state accessible by $S_0 \rightarrow T_1$ absorption.

Quantum Efficiencies. The simplification of eq 3 in computing the quantum yield ratio makes it possible to evaluate emission quantum yields resulting from excitation at a wavelength that partially or dominantly overlaps with the emission spectrum. Also with the absorption and excitation spectra in hand, emission quantum yields resulting from any excitation energies and quantum efficiencies between excited states can readily be computed and compared.

The large differences between emission quantum yields resulting from $S_0 \rightarrow S_1$ and $S_0 \rightarrow T_1$ excitations suggest a very small intersystem crossing quantum yield. From equation $\phi_{isc} = \phi_{P,S}/\phi_{P,T}$, the intersystem crossing quantum yield at 296 K is estimated to be 0.013−0.016. Thus, only 1.3−1.6% of the energy populating the singlet excited-state crossed over to the emitting state. In contrast, the ϕ_{isc} values at 77 K in a glassy matrix are in the range 0.07−0.5 for the various complexes (or the ϕ_{isc}^{-1} values in the range 2−14 in Table 1). These are much larger than those computed at 296 K and are expected, since more singlet excited states in the glassy matrix at 77 K are able to escape from collisional deactivation with the solvent and thereby undergo intersystem crossing to the triplet state.

The application of excitation spectra together with absorption spectra makes the evaluation of quantum efficiencies between excited states and the ground state available. The validity of eq 3 can be justified from a mathematical point of view. If we assume the emission spectra follow the Gaussian distribution described by

$$I(\nu) = \{B/[w(\pi/2)^{0.5}]\}e^{-2(\nu-\nu_{max})^2/w^2} \qquad (6)$$

where B is the total area under the emission spectrum and equals $\int I(\nu)\ \mathrm{d}\nu$, w equals 0.849 times the width of the peak at half-height, and ν_{max} is the energy at the peak. The peak intensity is written as

$$I_{max} = B/[w(\pi/2)^{0.5}] = \int I(\nu)\ \mathrm{d}\nu/[w(\pi/2)^{0.5}] \qquad (7)$$

Since $I_\lambda = I_{max}$, then eq 7 can be rewritten as

$$I_\lambda = \int I(\nu)\ \mathrm{d}\nu/[w(\pi/2)^{0.5}] \qquad (8)$$

or as

$$I_\lambda \propto \int I(\nu)\ \mathrm{d}\nu \qquad (9)$$

if w is treated as a constant. Therefore, the integrals used in eq 2 can be replaced by the intensities at the excitation wavelength, I_λ.

Theoretical Computation of Radiative Rate Constants. Radiative rate constants were calculated[15] for two of the complexes from the absorption and emission spectra using eq 10, where k_r is the radiative rate constant, g_l and g_u are the

$$k_r = 2.880 \times 10^{-9} n^2 <\nu e^{-3}> A\upsilon^{-1} (g_l/g_u) \int \epsilon\ \mathrm{d}\ln\nu \qquad (10)$$

degeneracies of lower and upper states, respectively; ϵ is the molar extinction coefficient; n is the refractive index of the medium; $<\nu e^{-3}>A\upsilon^{-1}$ is the ratio of integrals over the emission spectrum and was determined by eq 11; ν is the energy of

$$<\nu e^{-3}>A\upsilon^{-1} = \int I(\nu)\ \mathrm{d}\nu / \int \nu^{-3} I(\nu)\ \mathrm{d}\nu \qquad (11)$$

transition in cm^{-1}. Since the $S_0 \rightarrow T_1$ absorption bands overlapped considerably with the strong $S_0 \rightarrow S_1$ absorption bands, a correction was made by subtracting the tail of the stronger band from the $S_0 \rightarrow T_1$ absorption bands. The original spectra and corrected ones for Pt(bph)(dppm) and Pt(2-phq)-(dppm)(PF)6 are shown in Figure 3. The calculated k_r values were 2 orders of magnitude lower than the experimental k_r' values (Table 2). Since eq 10 holds for (i) strong transitions ($\epsilon = 8000$) and (ii) those having no large change in configuration of the excited states, it follows that the restrictions are maintained resulting in calculated values in disagreement with experimental ones.

Conclusions

The importance of direct singlet-to-triplet transitions can be summarized as follows. First, the $S_0 \rightarrow T_1$ absorption data along with emission spectra permit assignment of the nature of the lowest triplet state. Furthermore, efficiencies of intersystem crossing can be determined by quantitative $S_0 \rightarrow T_1$ absorption studies. Second, the long-lived triplet excited state may absorb suitable energy photons and be excited to higher energy triplet states. These multiphoton processes may result in higher energy states which transfer energy to other compounds where chemical reactions may be triggered. Third, since in most of the cases the triplet excited state lies lower in energy than the corresponding singlet excited state, direct population of the triplet excited state requires less energy, which, for the platinum complexes studied here, shifts the absorption into the visible region of the spectrum. Fourth, the efficiency of solar energy conversion is improved by eliminating energy loss through processes such as internal conversion and intersystem crossing.

Acknowledgment. The authors thank the Office of Basic Energy Sciences of the United States Department of Energy for support and the National Science Foundation for the laser equipment.

IC980324C

(15) Strickler, S. J.; Berg, R. J. *J. Chem. Phys.* **1962**, *37*, 814.